IOPscience iopscience.iop.org

Home Search Collections Journals About Contact us My IOPscience

The reaction process of hydrogen absorption and desorption on the nanocomposite of hydrogenated graphite and lithium hydride

This content has been downloaded from IOPscience. Please scroll down to see the full text.

2009 Nanotechnology 20 204021

(http://iopscience.iop.org/0957-4484/20/20/204021)

View the table of contents for this issue, or go to the journal homepage for more

Download details:
This content was downloaded by: davidfojt
IP Address: 80.215.91.216
This content was downloaded on 22/05/2017 at 11:11

Please note that terms and conditions apply.

You may also be interested in:

Synthesis, characterization, and reversible hydrogen sorption study of sodium-doped fullerene
Douglas A Knight, Joseph A Teprovich Jr, Andrew Summers et al.

Nanostructured Ti-catalyzed MgH2 for hydrogen storage
H Shao, M Felderhoff, F Schüth et al.

The synthesis and hydrogen storage properties of pure nanostructured Mg2FeH6
Xuanzhou Zhang, Rong Yang, Jianglan Qu et al.

Novel catalytic effects of fullerene for LiBH4 hydrogen uptake and release
Matthew S Wellons, Polly A Berseth and Ragaiy Zidan

The long-term hydriding and dehydriding stability of the nanoscale LiNH2 + LiH hydrogenstorage system
William Osborn, Tippawan Markmaitree and Leon L Shaw

Size effects on the hydrogen storage properties of nanoscaffolded Li3BN2H8
Hui Wu, Wei Zhou, Ke Wang et al.

The kinetic enhancement of hydrogen cycling in NaAlH4 by melt infusion into nanoporouscarbon aerogel
Robert D Stephens, Adam F Gross, Sky L Van Atta et al.

Hydrogen storage and cycling properties of a vanadium decorated Mg nanoblade array on aTi coated Si substrate
Yuping He and Yiping Zhao

Nanotechnology **20** (2009) 204021 (5pp) doi:10.1088/0957-4484/20/20/204021

The reaction process of hydrogen absorption and desorption on the nanocomposite of hydrogenated graphite and lithium hydride

Hiroki Miyaoka, Takayuki Ichikawa[1] and Yoshitsugu Kojima

Institute for Advanced Materials Research, Hiroshima University, 1-3-1Kagamiyama, Higashi-Hiroshima, Hiroshima 739-8530, Japan

E-mail: tichi@hiroshima-u.ac.jp

Received 22 September 2008, in final form 9 January 2009
Published 24 April 2009
Online at stacks.iop.org/Nano/20/204021

Abstract
The lithium–carbon–hydrogen (Li–C–H) system is composed of hydrogenated nanostructural graphite ($C^{nano}H_x$) and lithium hydride (LiH). $C^{nano}H_x$ is synthesized by ball-milling of graphite under a hydrogen atmosphere. In this work, the reaction process of hydrogen absorption and desorption on the Li–C–H system is investigated. The $C^{nano}H_x$–LiH composite can desorb about 5.0 mass% of hydrogen at 350 °C with the formation of Li_2C_2 until the second cycle. However, the hydrogen desorption amount significantly decreases from the third cycle. Furthermore, it is shown by using gas chromatography that a considerable amount of hydrocarbons is desorbed during the rehydrogenation process. These results indicate that the amount of reaction between the polarized C–H groups in $C^{nano}H_x$ and LiH is reduced due to a decrease in the C–H groups by losing carbon atoms under the hydrogen absorption and desorption cycles.

1. Introduction

Recently, hydrogen storage and transportation are being studied all over the world as the key technology to establish clean and renewable energy systems for a sustainable society. In the case of an on-board application for a vehicle, hydrogen should be stored in a compact, light, safe and reasonable vessel. At present, high-pressure hydrogen gas, liquid hydrogen and hydrogen storage materials are considered as the hydrogen storage techniques. Among them, hydrogen storage materials can safely store a higher density of hydrogen compared to the gaseous and liquid hydrogen storage systems. Therefore, the systems using hydrogen storage materials are considered as the most suitable technique [1–5]. In particular, a great deal of attention has been paid to materials based on the light elements because these materials are expected to realize high gravimetric and volumetric densities of hydrogen [6–8].

Carbon is one of the attractive light elements because of its abundance and low cost. Therefore, a lot of carbon-based materials have been investigated as a hydrogen storage material since Dillon *et al* reported on single-walled carbon nanotubes in 1997 [9]. Among them, the hydrogenated nanostructural graphite ($C^{nano}H_x$) can stably store about 4 mass% of hydrogen. The hydrogen ab/desorption properties of $C^{nano}H_x$ have been investigated so far [10–15]. $C^{nano}H_x$ is synthesized from graphite by the ball-milling method under hydrogen atmosphere. With respect to the hydrogen absorption site in this product, the hydrogen atoms are chemisorbed as stable C–H bonds at the graphene edges and defects induced by ball-milling [16–18]. On the other hand, this product needs a high temperature of more than 700 °C to release the hydrogen and it desorbs a considerable amount of hydrocarbons, methane (CH_4) and ethane (C_2H_6), together with hydrogen. Furthermore, it is quite difficult to recharge this product with hydrogen under moderate conditions of pressure and temperature for on-board applications. In order to improve the hydrogen absorption and desorption properties of $C^{nano}H_x$, Ichikawa *et al* have paid attention to the chemical reaction between NH_3 and LiH, which is one of the elementary reactions in the Li–N–H system [19]. This reaction proceeds even at room temperature, and the system

[1] Author to whom any correspondence should be addressed.

 © 2009 IOP Publishing Ltd Printed in the UK

releases hydrogen. This indicates that the stable ionic crystal of LiH is destabilized by reacting with a polar molecule such as ammonia (NH_3) to form lithium amide ($LiNH_2$). On the analogy of this reaction, a hydrogen storage system using a reaction between $C^{nano}H_x$ and LiH has been designed, where the C–H groups in $C^{nano}H_x$ are polarized (similar to NH_3), as is clear from the existence of the IR-active modes corresponding to the C–H bonding [18]. Actually, it is clarified that the hydrogen absorption and desorption properties of $C^{nano}H_x$ is improved by synthesizing the nanocomposites with LiH. The $C^{nano}H_x$–LiH composite desorbs hydrogen around 350 °C by the interaction between both components to form lithium carbide (Li_2C_2). Furthermore, the dehydrogenated composites can be recharged with hydrogen of about 5.0 mass% at 350 °C under hydrogen pressure of 3.0 MPa [20]. In fact, the Li–C–H system was discovered in 2005, yet the hydrogen absorption and desorption mechanisms (reaction paths) on this system are not fully clarified to date. The Li–C–H system would be categorized as a new hydrogen storage system because the hydrogen absorption and desorption reactions would be induced by a characteristic interaction between the polarized C–H groups in $C^{nano}H_x$ and LiH, which has not been reported so far. Therefore, the hydrogen absorption and desorption reactions are quite different from conventional hydrogen storage systems, indicating that an understanding of the hydrogen ab/desorption properties of the systems could lead to the design of a new hydrogen storage system with further high performance.

In this paper, the cyclic hydrogen absorption and desorption properties of the $C^{nano}H_x$–LiH composite are investigated as fundamental research from the thermodynamic and structural points of view. On the basis of these results, the hydrogen absorption and desorption reaction process in this system are discussed.

2. Experimental procedures

2.1. Sample preparation

The hydrogenated nanostructural graphite ($C^{nano}H_x$) was synthesized from graphite powder (99.999%, Stream Chemicals) by the vibrating ball-mill apparatuses (Seiwa Giken Co. Ltd, RM-10). Graphite of 300 mg and 20 ZrO_2 balls with 8 mm in diameter were put into a milling vessel made of Cr steel (Umetoku Co. Ltd, SKD-11). Then, ball-milling was performed under 1.0 MPa H_2 pressure at room temperature for 80 h.

In order to synthesize the composites, $C^{nano}H_x$ and LiH (95%, Aldrich) were mechanically milled for 2 h under a 1.0 MPa H_2 atmosphere at room temperature by using a rotating ball-mill apparatus (Fritsch, P7). The molar ratio of $C^{nano}H_x$ and LiH was chosen to be 2:1 as a suitable composition from previous studies [21].

The dehydrogenating and rehydrogenating treatments for the $C^{nano}H_x$–LiH composites were performed at 350 °C for 8 h under high vacuum condition and 3.0 MPa H_2 pressure in a reactor made of steel, respectively.

All the samples were handled in a glove box (Miwa MFG, MP-P60W) filled with purified Ar gas (>99.9999%) to avoid oxidation.

2.2. Experimental techniques

Thermal gas desorption properties of the composites were examined by a thermal desorption mass spectroscopy (TDMS) (Anelva, M-QA200TS) connected to thermogravimetry (TG) (Rigaku, TG8120). This equipment is installed inside the glove box to minimize oxidation and water adsorption by the samples. In the thermal analysis, high purity helium (He) gas (>99.9999%) was flowed as a carrier gas and the heating rate was fixed at 5 °C min^{-1}. In the TDMS measurements for all the samples, some fragments related to desorption gases such as H_2, CH_4 and C_2H_6 were monitored as desorption gases.

Structures of the composites were investigated by x-ray diffraction (XRD) measurement (Rigaku, RINT-2100, Cu Kα radiation), where all the samples were covered by a polyimide sheet (Kapton®, Du Pont-Toray Co., Ltd) in the glove box to avoid oxidation during the XRD measurement.

The remaining gases in the reactor used to rehydrogenate the composites by heat treatment were determined by gas chromatography (GC) (Shimazu, GC-14B). After the rehydrogenating treatment, the reactor was connected to the GC apparatus. In the GC measurement, the temperature of the column was set to be 100 °C, and high purity Ar gas was flowed as a carrier gas.

3. Results and discussion

Figure 1 shows the TDMS and TG profiles of the composites after synthesizing and after each cycle of hydrogen absorption/desorption up to five times, where mass numbers 2, 16 and 28 are assigned to H_2, CH_4 and C_2H_6, respectively. In the TDMS profile of the as-synthesized composite shown in figure 1, the intensities of CH_4 and C_2H_6 are enlarged ten times, indicating that this composite desorbs the hydrogen around 350 °C with a small amount of hydrocarbon desorption. The hydrogen desorption peak temperature at 350 °C is lower than the decomposition temperatures of $C^{nano}H_x$ and LiH themselves. The TG profile of the as-synthesized composite (dashed and dotted lines in figure 1) reveals a weight loss of about 10.0 mass% during heating up to 500 °C. This weight loss is mostly due to hydrogen gas, but includes a small amount of hydrocarbon desorption. After the dehydrogenation and rehydrogenation cycles, the hydrogen desorption profile of the composites reveals a two-peak structure, where those peaks corresponding to hydrogen desorption are located around 350 and 450 °C. These hydrogen desorption temperatures are still lower than the decomposition temperature of each component, indicating that the hydrogen desorption of cycled composites could take place by the interaction between the polarized C–H groups and LiH. In fact, it is clarified by neutron diffraction measurements that the C–H bonds are formed during the rehydrogenation process [20]. It should be noticed that only hydrogen is desorbed from the rehydrogenated composites without any hydrocarbon emission, suggesting that the hydrogen absorption state of the hydrogen recharged composite is slightly different from that of the as-synthesized composite. The hydrogen desorption peak around 450 °C in the TDMS profile may be caused by the slow reaction

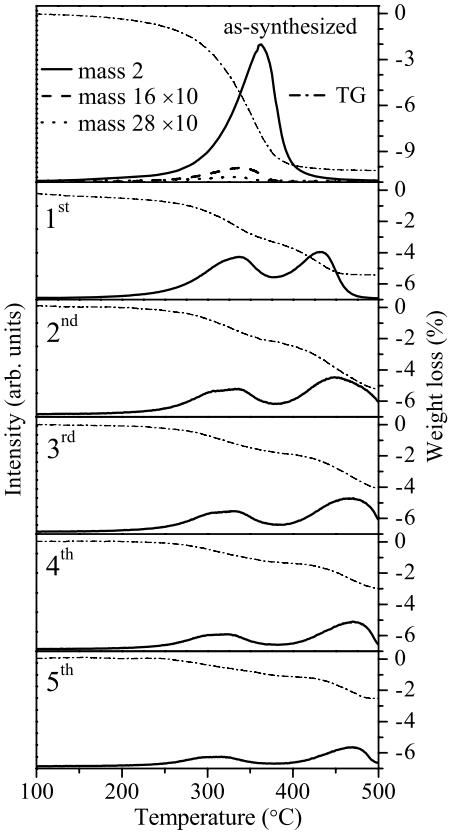

Figure 1. TDMS and TG profiles (dashed and dotted lines) of the $C^{nano}H_x$–LiH composites after synthesizing and rehydrogenation five times, where masses 2, 16 and 28 correspond to H_2, CH_4, and C_2H_6, respectively.

kinetics because this peak almost disappeared in the TDMS after the second dehydrogenation at 350 °C. The first and second rehydrogenated composites can desorb 5.0 mass% of hydrogen, as shown in their TG profiles. However, the hydrogen desorption amount gradually decreases with hydrogen ab/desorption cycles after the third rehydrogenation although the shapes of the hydrogen desorption profiles are almost unchanged.

The structural change with hydrogenation and dehydrogenation cycles was examined by XRD measurements. The XRD profiles of the composite after synthesis and after each dehydrogenation and rehydrogenation treatment are shown in figure 2. As a reference, the XRD profiles of LiH (PDF #65-2897) and Li_2C_2 (PDF #21-0484) in the database are shown. In the XRD profile of the as-synthesized composite in figure 2(a), diffraction peaks corresponding to a LiH phase are observed and no other peaks related to carbon appear due to the nanostructural feature. After the first dehydrogenation treated at 350 °C for 8 h, the LiH phase disappears. On the other hand, new diffraction peaks assigned to Li_2C_2 appear, as shown in figure 2(b), although the peaks are quite small. By the first rehydrogenation at 350 °C for 8 h under H_2 pressure of 3 MPa, the Li_2C_2 phase disappears and then the LiH phase is recovered, as shown in figure 2(a). With the re/dehydrogenation treatments after the third cycle, it is clearly found that the peaks assigned to LiH remain in the dehydrogenating sample. The diffraction peaks corresponding to Li_2C_2 are grown by the second dehydrogenation treatment: however they gradually decrease from the third cycle. These results indicate that the formation of Li_2C_2 due to the interaction between the polarized C–H groups in $C^{nano}H_x$ and LiH decreases from the third cycle. This phenomenon is quite consistent with the decrease in the hydrogen desorption amount after the third cycle obtained by TG.

In order to understand the hydrogen absorption process in further detail, the gases remaining in the reactor, which are used for the rehydrogenation of the composite by heat treatment at 350 °C for 8 h under 3 MPa of H_2, are examined by GC after each rehydrogenation. The gas chromatograms

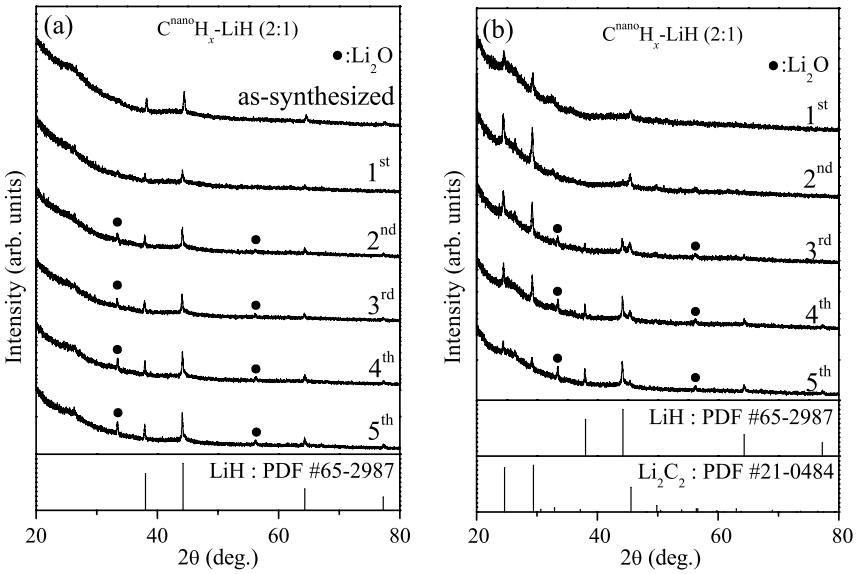

Figure 2. XRD profiles of (a) the hydrogenated and (b) the dehydrogenated $C^{nano}H_x$–LiH composites at room temperature after each dehydrogenating and rehydrogenating treatment. The XRD profiles of LiH and Li_2C_2 are referred to from the database (PDF #65-2897 and PDF #21-0484).

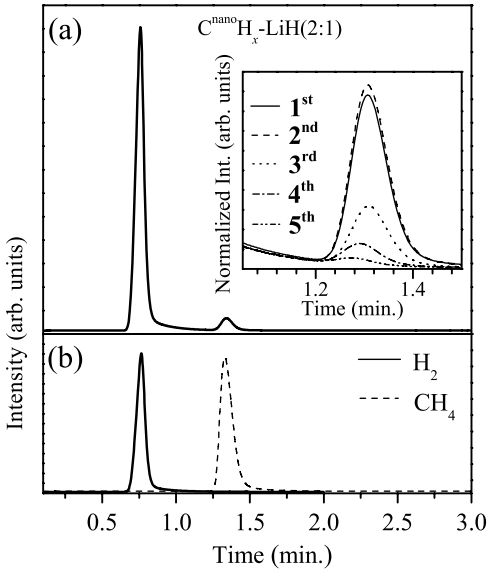

Figure 3. (a) The chromatograms of the gases remaining in the reactor after each rehydrogenation of the $C^{nano}H_x$–LiH composite by heat treatment at 350 °C for 8 h under 3 MPa of hydrogen, and the second peaks observed after each rehydrogenation are shown in the inset, in which the peak intensity is normalized by the intensity of the first peak. (b) The chromatograms of H_2 and CH_4 are used as reference.

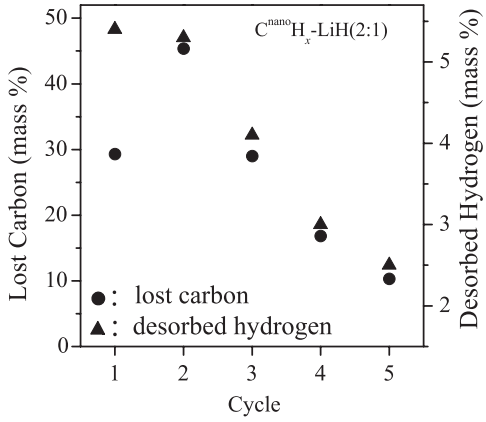

Figure 4. Amount of carbon lost during each rehydrogenation of the $C^{nano}H_x$–LiH composite and the hydrogen desorbed from each rehydrogenated composite as a function of the hydrogen ab/desorption cycle, which is estimated from the results from GC and TG, respectively.

for the composites are shown in figure 3(a) and the results of GC for H_2 and CH_4 gases are appended in figure 3(b) as references. All the chromatograms of the composites show two peaks at different retention times. The respective peaks are assigned to H_2 and CH_4 because the positions of the peaks are quite consistent with those of the reference. The results indicate that the hydrocarbons, mainly CH_4, are desorbed with decomposition of Li_2C_2 by recharging the composite with hydrogen, where a quite small amount of ethane C_2H_6 is also observed in the GC. As shown in the inset of figure 3(a), the normalized intensity of the peak ascribed to CH_4 is gradually weakened by the third rehydrogenation, in which the normalization of the peaks is carried out by using the intensity of H_2.

Figure 4 shows the amount of carbon lost as hydrocarbons during each rehydrogenating treatment as a function of the number of hydrogen ab/desorption cycles, assuming that the desorbed gas is only CH_4. Figure 4 also shows the amount of hydrogen gas desorbed from each rehydrogenated composite. The amount of carbon in CH_4 and H_2 are estimated respectively by GC and TG. At the first cycle, about 29.0 mass% of the carbon atoms is desorbed as CH_4 and 5.0 mass% of H_2 is desorbed from the composite. The amount of lost carbon reaches up to 45.4 mass% at the second hydrogen recharge, and gradually decreases with hydrogenating treatment from the third cycle. As shown in figure 4, the decrease in hydrogen desorption amount also starts from the third cycle. The variation in the amount of lost carbon and desorbed hydrogen by the hydrogenation and rehydrogenation cycles is quite consistent with each other. Therefore, the results of GC indicate that the hydrogen absorption and desorption properties of the composite are strongly related to hydrocarbon desorption during the hydrogen recharging process. From the above experimental facts and the following four assumptions,

(1) the quite small amount of hydrocarbon desorption from the as-synthesized composite can be ignored (figure 1),
(2) the hydrogenated state of the ball-milled graphite in the composite after rehydrogenation is defined as $C^{nano}H_y$ because the rehydrogenated state of the composite is different from that of $C^{nano}H_x$ in the as-synthesized composite, and the $H/C = y$ is not changed with the cycled treatments,
(3) half of the carbons in the Li_2C_2 is desorbed as CH_4 gas with recharging hydrogen, and
(4) H_2 or CH_4 desorbed by each treatment is removed from the system,

it is expected that the hydrogen absorption and desorption reaction in the Li–C–H system with the cycles of hydrogenation and dehydrogenation treatment is expressed as follows:

Initial desorption: $2C^{nano}H_x + LiH$

$$\rightarrow C^{nano} + \frac{1}{2}Li_2C_2 + \left(\frac{4x+2}{4}\right)H_2\uparrow, \quad (1)$$

First cycle: (abs.) $C^{nano} + \frac{1}{2}Li_2C_2 + \left(\frac{3y+6}{4}\right)H_2$

$$\rightarrow \tfrac{3}{2}C^{nano}H_y + \tfrac{1}{2}CH_4\uparrow + LiH, \quad (2)$$

(des.) $\frac{3}{2}C^{nano}H_y + LiH$

$$\rightarrow \frac{1}{2}C^{nano} + \frac{1}{2}Li_2C_2 + \left(\frac{3y+2}{4}\right)H_2\uparrow, \quad (3)$$

Second cycle: (abs.) $\frac{1}{2}C^{nano} + \frac{1}{2}Li_2C_2 + \left(\frac{2y+6}{4}\right)H_2$

$$\rightarrow C^{nano}H_y + \tfrac{1}{2}CH_4\uparrow + LiH, \quad (4)$$

(des.) $C^{nano}H_y + LiH$

$$\rightarrow \frac{1}{2}Li_2C_2 + \left(\frac{2y+2}{4}\right)H_2\uparrow, \quad (5)$$

Third cycle: (abs.) $\frac{1}{2}Li_2C_2 + \left(\frac{y+6}{4}\right)H_2$

$$\rightarrow \tfrac{1}{2}\left(C^{nano}H_y + CH_4\uparrow\right) + LiH, \quad (6)$$

(des.) $\frac{1}{2}C^{nano}H_y + LiH$

$$\rightarrow \frac{1}{4}Li_2C_2 + \left(\frac{y+1}{4}\right)H_2\uparrow + \frac{1}{2}LiH, \quad (7)$$

Fourth cycle: (abs.) $\frac{1}{4}Li_2C_2 + \frac{1}{2}LiH + \left(\frac{y+6}{8}\right)H_2$

$$\rightarrow \tfrac{1}{4}\left(C^{nano}H_y + CH_4\uparrow\right) + LiH, \quad (8)$$

(des.) $\frac{1}{4}C^{nano}H_y + LiH$

$$\rightarrow \frac{1}{8}Li_2C_2 + \left(\frac{y+1}{8}\right)H_2\uparrow + \frac{3}{4}LiH, \quad (9)$$

Fifth cycle: (abs.) $\frac{1}{8}Li_2C_2 + \frac{3}{4}LiH + \left(\frac{y+6}{16}\right)H_2$

$$\rightarrow \tfrac{1}{8}\left(C^{nano}H_y + CH_4\uparrow\right) + LiH, \quad (10)$$

(des.) $\frac{1}{8}C^{nano}H_y + LiH$

$$\rightarrow \frac{1}{16}Li_2C_2 + \left(\frac{y+1}{16}\right)H_2\uparrow + \frac{7}{8}LiH. \quad (11)$$

In this reaction model, the non-reacted LiH remains from the third cycle. The hydrogen ab/desorption reactions of the Li–C–H system from the third cycles can be described by the following equations ($n = 1, 2, 3$, etc):

nth cycle:

(abs.) $\frac{1}{2^n}Li_2C_2 + \left(\frac{2^{n-1}-1}{2^{n-1}}\right)LiH + \left(\frac{y+6}{2^{n+1}}\right)H_2$

$$\rightarrow \frac{1}{2^n}\left(C^{nano}H_y + CH_4\uparrow\right) + LiH, \quad (12)$$

(des.) $\frac{1}{2^n}C^{nano}H_y + LiH \rightarrow \frac{1}{2^{n+1}}Li_2C_2 + \left(\frac{y+1}{2^{n+1}}\right)H_2\uparrow$

$$+ \left(\frac{2^n-1}{2^n}\right)LiH. \quad (13)$$

Therefore, it is considered that the model of hydrogen absorption/desorption reactions of the Li–C–H system expressed by the above equations would describe the experimental results obtained in this work.

4. Summary

In order to characterize the hydrogen absorption and desorption process of the Li–C–H system, thermal and structural analyses were carried out for the $C^{nano}H_x$–LiH composite cycled by hydrogenation/dehydrogenation at 350 °C.

The composite is able to desorb and absorb 5.0 mass% of hydrogen until the second cycle, and then Li_2C_2 is formed as the dehydrogenated state. However, the hydrogen desorption amount gradually decreases from the third cycle. From the results of the XRD measurements, it is also clear that the non-reacted LiH gradually increases from the third cycle. In the hydrogen absorption process, a considerable amount of hydrocarbon desorption is observed by GC, indicating that carbon atoms in the composite are lost with each hydrogen recharging process. Therefore, it is considered that the decrease in the hydrogen desorption amount observed by TG is caused by desorbing hydrocarbons with the decomposition of Li_2C_2 under rehydrogenation, or in other words, the amount of hydrogen desorption reaction between the polarized groups composed of C–H bonds and LiH are gradually reduced due to the decrease in C–H groups by the loss of the carbon atoms with rehydrogenation.

The Li–C–H system would be recognized as one of the attractive systems for hydrogen storage. However, it is confirmed by this work that the hydrocarbon desorption during the hydrogen recharging process is essentially a problem for this system, because it reduces the hydrogen absorption amount. For practical use as a hydrogen storage system, an improvement, e.g. usage of a catalyst or scaffold, is needed to prevent hydrocarbon desorption during hydrogenation.

Acknowledgments

This work was partially supported by the project 'Advanced Fundamental Research Project on Hydrogen Storage Materials' of the New Energy and Industrial Technology Development Organization (NEDO) and Research Fellowships of the Japan Society for the Promotion of Science for young Scientists (JSPS). The authors gratefully acknowledge Dr Shigehito Isobe and Mr Satoshi Hino for fruitful discussions of this work.

References

[1] Schlapbach L and Züttel A 2001 *Nature* **414** 353
[2] Akiba E 1999 *Curr. Opin. Solid State Mater. Sci.* **4** 267
[3] Sandrock G 1999 *J. Alloys Compounds* **295** 877
[4] Grochala W and Edwards P P 2004 *Chem. Rev.* **104** 1283
[5] Züttel A 2007 *Mitigation and Adaptation Strategies for Global Change* vol 12 (The Netherlands: Springer) p 343
[6] Schüth F, Bogdanović B and Felderhoff M 2004 *Chem. Commun.* 2243
[7] Züttel A 2004 *Naturwissenschaften* **91** 157
[8] Orimo S I, Nakamori Y, Eliseo J R, Zuttel A and Jensen C M 2007 *Chem. Rev.* **107** 4111
[9] Dillon A C, Jones K M, Bekkedahl T A, Kiang C H, Bethune D S and Heben M J 1997 *Nature* **386** 377
[10] Orimo S, Majer G, Fukunaga T, Züttel A, Schlapbach L and Fujii H 1999 *Appl. Phys. Lett.* **75** 3093
[11] Orimo S, Matsushima T, Fujii H, Fukunaga T and Majer G 2001 *J. Appl. Phys.* **90** 1545
[12] Chen D M, Ichikawa T, Fujii H, Ogita N, Udagawa M, Kitano Y and Tanabe E 2003 *J. Alloys Compounds* **354** L5
[13] Majer G, Stanik E and Orimo S 2003 *J. Alloys Compounds* **356** 617
[14] Ichikawa T, Chen D M, Isobe S, Gomibuchi E and Fujii H 2004 *Mater. Sci. Eng.* B **108** 138
[15] Stanik E, Majer G, Orimo S, Ichikawa T and Fujii H 2005 *J. Appl. Phys.* **98** 044302
[16] Fukunaga T, Itoh K, Orimo S and Aoki K 2004 *Mater. Sci. Eng.* B **108** 105
[17] Itoh K, Miyahara Y, Orimo S, Fujii H, Kamiyama T and Fukunaga T 2003 *J. Alloys Compounds* **356** 608
[18] Ogita N, Yamamoto K, Hayashi C, Matsushima T, Orimo S, Ichikawa T, Fujii H and Udagawa M 2004 *J. Phys. Soc. Japan* **73** 553
[19] Ichikawa T, Hanada N, Isobe S, Leng H Y and Fujii H 2004 *J. Phys. Chem.* B **108** 7887
[20] Miyaoka H, Itoh K, Fukunaga T, Ichikawa T, Kojima Y and Fuji H 2008 *J. Appl. Phys.* **104** 053511
[21] Ichikawa T, Fujii H, Isobe S and Nabeta K 2005 *Appl. Phys. Lett.* **86** 241914